Journal of Pharmaceutical and Biomedical Analysis 47 (2008) 596–602

Contents lists available at ScienceDirect

Journal of Pharmaceutical and Biomedical Analysis

journal homepage: www.elsevier.com/locate/jpba

Acrolein sequestering ability of the endogenous tripeptide glycyl-histidyl-lysine (GHK): Characterization of conjugation products by ESI-MS^n and theoretical calculations

Giangiacomo Beretta[a,*], Emanuele Arlandini[a], Roberto Artali[a], Josep M. Garcia Anton[b], R. Maffei Facino[a]

[a] *Istituto di Chimica Farmaceutica e Tossicologica "Pietro Pratesi", University of Milan, Faculty of Pharmacy, Via Mangiagalli 25, 20133 Milan, Italy*
[b] *Lipotec S.A.Isaac Peral, 1, 08850 Gavà, Barcelona, Spain*

ARTICLE INFO

Article history:
Received 17 December 2007
Received in revised form 6 February 2008
Accepted 8 February 2008
Available online 10 March 2008

Keywords:
GHK
Acrolein
Quenching ability
Adducts
ESI-MS/MS
Computational studies

ABSTRACT

Acrolein (ACR) is a well-known carbonyl toxin produced by lipid peroxidation of polyunsaturated fatty acids, which is involved in several life-threatening pathologies such as Alzheimer disease, arteriosclerosis, diabetes, and nephropathy.

The aim of this work was to study the quenching ability of the endogenous tripeptide glycyl-histidyl-lysine (GHK), a liver cell growth factor isolated from human plasma, towards the electrophilic aldehyde ACR and to characterize the reaction products by electrospray mass spectrometry (ESI-MS/MS infusion experiments; positive ion mode). The reaction of ACR (30 μM) with GHK (0.1, 0.25, 0.5, 1.0 mM) was followed by measuring aldehyde consumption by reverse-phase HPLC (phosphate buffer, pH 7.4); after 4 h, when the aldehyde had completely disappeared; the reaction products were checked by ESI-MS/MS. Several products were detected in the GHK + ACR reaction (1:1). This indicates a complex reaction cascade involving the sequential addition of ACR (up to 3 mol) to the tripeptide GHK and, in particular, to the ε-amino group of the lysine residue and to the N^{τ} and N^{π} of the histidine moiety. The Michael addition of two molecules of ACR to the ε-amino group of the lysine residue is followed by aldol condensation and dehydration to give the *N*-(3-formyl-3,4-dehydropiperidino) derivative.

The results confirm that the ESI-MS/MS approach in a direct infusion experiment permits rapid profiling of the products of the GHK + ACR reaction. They firstly point to the potential medicinal use of GHK in the prevention of carbonyl stress-linked pathologies, and – second – help shed light on the physiological role of this histidine-containing tripeptide which is claimed to be an endogenous growth factor, but has never been shown to be an ACR quencher.

1. Introduction

Lipid peroxidation of polyunsaturated fatty acids (PUFAs) is responsible for the formation of a burst of cytotoxic α,β-unsaturated aldehydes (4-hydroxy-nonenal, HNE; acrolein, ACR; crotonaldehyde) which, together with malondialdehyde, glyoxal and methylglyoxal, through the breakdown of sugars, are the causes of a range of human diseases associated with oxidative stress. This process, which takes place basically in inflammatory diseases, amplifies oxidative cell injury by modifying key cell proteins, where the main targets for reactions with electrophilic aldehydes are the nucleophilic ε-amino group of lysine, the SH group of cysteine and the imidazole group of histidine, and DNA bases through either Michael or Schiff base adduction [1].

ACR is a cytotoxic α,β-unsaturated three-carbon aldehyde and a major product of organic combustion including tobacco smoking. It is formed endogenously from the polyamine metabolism, lipid peroxidation and threonine oxidation [2,3]. ACR levels are high in several diseases such as atherosclerosis, Alzheimer disease and diabetes [4], and it plays a role in the progression of atherosclerosis through COX-2 induction [5].

In a recent study using an experimental and theoretical approach, we reported that the endogenous tripeptide glycyl-histidyl-lysine (GHK), established as a human growth factor [6], has marked ability to remove the α,β-unsaturated aldehyde 4-hydroxy-nonenal (HNE), the prototype of the biologically relevant α,β-unsaturated aldehydes [7].

* Corresponding author. Tel.: +39 02 503 19309; fax: +39 02 503 19359.
E-mail address: giangiacomo.beretta@unimi.it (G. Beretta).

0731-7085/$ – see front matter © 2008 Elsevier B.V. All rights reserved.
doi:10.1016/j.jpba.2008.02.012

Pursuing our interest in defining the biological role of histidine-containing oligopeptides, and possibly discovering new oligopeptides to attenuate the increased aldehyde load in different pathologies, we studied the quenching ability of the basic tripeptide GHK towards ACR and characterized the structure of the adducts formed by mass spectrometry.

First, we investigated the kinetics of ACR (30 μM) consumption by GHK (molar ratios 1:3, 1:8, 1:17, 1:30) in physio-mimetic conditions, using an HPLC method; then we studied the structure of intermediates and final adducts by ESI-MS and ESI-MS/MS experiments in direct infusion, to profile the cascade of events leading to removal of the toxic aldehyde.

In addition we made a theoretical study of the effects of the molecular dynamics of the intermediates on the formation and structures of the different ACR–GHK adducts. The formation of the mono- and pluri-ACR/GHK adducts and their structural features can shed light on the biological importance of the quenching reaction between GHK and ACR and explain GHK's physiological role *in vivo*. This may have synergy of action with the endogenous GSH, the main ACR detoxifying tool, in preserving the cell thiol reservoir [3]. GHK might therefore offer an attractive therapeutic intervention in pathological situations where ACR levels are markedly elevated (e.g. atheromatous plaque, end-stage renal disease).

2. Experimental

2.1. Chemicals

All chemicals and reagents were of analytical grade and purchased from Sigma–Fluka–Aldrich Chemical Co. (Milan, Italy). HPLC grade and analytical grade organic solvents were purchased from Merck (Bracco, Milan, Italy). HPLC grade water was prepared with a Milli-Q water purification system. Glycyl-L-histidyl-L-lysine (GHK) was a kind gift from Lipotec S.A. (Barcelona, Spain). Acrolein (ACR) was from Sigma (Milan, Italy).

2.2. GHK incubation with ACR and HPLC analysis

HPLC analysis was done as previously reported [8]. Briefly, ACR (30 μM in 1 mM phosphate buffer, pH 7.4) was incubated with 0.1, 0.25, 0.5, 1 mM GHK (PBS, 1 mM, pH 7.4) at 37 °C. At different incubation times (1, 2, 3, 4 h) samples were withdrawn and directly analyzed by HPLC to measure ACR consumption.

ACR was determined by reverse-phase HPLC, using an HP1050 series instrument (Hewlett-Packard, Milan, Italy) equipped with a quaternary pump system, an autosampler, a UV–vis diode-array programmable detector operating at 223 nm, an on-line degasser and a LC^{3D} Chemstation.

Analyses were done by reverse-phase elution with a Supelco LC-18 column (250 mm × 4.6 mm i.d., particle size 5 μm). The mobile phase (isocratic elution) was 70% A (water/acetonitrile/formic acid; 9:1:0.01 v/v) and 30% B (water/acetonitrile; 1:9 v/v) and was delivered at a flow rate of 1 mL/min. Retention time for ACR was 4.3 min.

2.3. ESI-MS/MS analysis

ESI-MS and ESI-MS/MS analyses were done on a Thermo Finnigan LCQ Advantage (Thermoquest, Milan, Italy) ion trap mass spectrometer operating under the following conditions: capillary temperature 250 °C; ionization voltage 5 kV; heated capillary voltage 12.5 V; sheath gas flow rate 2 L/min. The flow rate of the nitrogen nebulizer gas was 0.5 L/min.

Samples (1:1 molar ratio, 4 h incubation) were diluted 1:5 with a water/acetonitrile mixture (70:30), then injected into the mass spectrometer using a Harvard syringe pump at a flow rate of 25 μL/min. Spectra were acquired in positive ion mode, with a scan range m/z 100–1000 (scan rate 0.5 scans/s).

For collision-induced dissociation (CID) experiments the relative collision energy was set at 30% (optimized using the LCQ-XCalibur software), the isolation width at 1 m/z, and helium as collision gas.

2.4. Computation methods

A detailed modeling study of GHK was done through theoretical calculations in two steps. First, the conformational space was completely explored using the molecular dynamics module of TINKER [9,10]. Peptides were soaked in a water box containing TIP3P water molecules, then simulated for 1.0 ns at a constant temperature of 298 K. The time step was 1.0 fs and the system was saved every 1.0 ps, giving a set of 1000 conformations for both peptides. The resulting molecular conformations were then optimized with respect to all the torsion angles and convergence was assumed when the energy changes in two successive cycles of the minimization procedure were less than 0.5 kcal/mol. An MM2 force-field was used for the conformational energies, and atomic charges were determined with the MOPAC 7.0 semi-empirical molecular orbital software [9]. All the minimum energy conformations were then re-optimized using the default scheme in Gaussian03 at the B2LYP/6-31G(d) [11] level of theory. The solvatation energy was calculated with continuum solvent models (PCM) to take account of the strong influence of water on the behavior of these compounds.

3. Results and discussion

3.1. GHK/ACR-sequestering ability

Fig. 1 reports the chemical structures of ACR and GHK. The carbonyl-quenching activity of GHK against a fixed concentration of ACR (30 μM) was evaluated at the different ACR:GHK molar ratios (1:3, 1:8, 1:17, 1:30) by monitoring the disappearance of the peak with RT 4.3 min at 1-h intervals. No additional peaks due to GHK and ACR degradation products were observed. ACR alone was stable throughout the experiment, thus excluding any loss by evaporation (b.p.$_{ACR}$ 57 °C).

Fig. 2 reports the time-course of the ACR-sequestering ability of GHK, showing that in a physio-mimetic buffer system (phosphate buffer, pH 7.4), GHK quenches ACR in a time- and dose-dependent fashion due to the adduction of ACR to the nucleophilic centers of the peptide (gly and lys amino groups and His imidazole).

After 4 h incubation, the ACR peak was no longer detectable in the HPLC chromatograms, indicating complete quenching.

Preliminary NMR investigations were done on the reaction mixture of ACR and GHK at equimolecular concentrations (the concentrations *in vivo* in plasma in physiological situations are

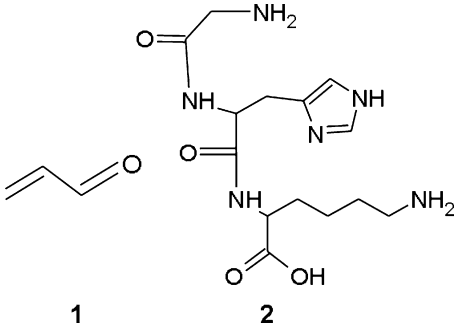

Fig. 1. Chemical structures of ACR and GHK.

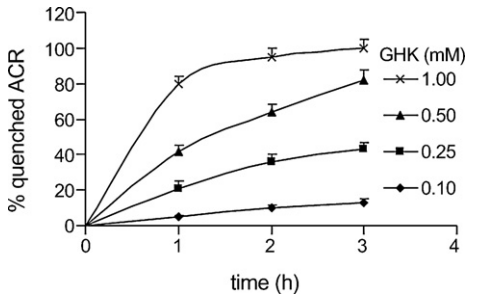

Fig. 2. ACR sequestering ability of GHK. Mean ± S.D. of five independent experiments. ACR (30 μM) was incubated in phosphate buffer, pH 7.4, with GHK at different concentrations. ACR consumption was determined by reverse-phase HPLC.

~0.3 μM for GHK and ~0.1–0.3 μM for ACR [6,12]). After 4 h incubation there was a complex mixture of adduction products, too complicated for direct NMR analysis (data not shown). The adducts were therefore characterized structurally by positive ion mode ESI-MS^n in direct infusion.

3.2. ESI-MS and ESI-MS/MS analyses of GHK/ACR adducts

To define the reactivity of GHK against ACR and the generation of ACR adducts, we first explored the GHK fragmentation pathway by ESI-MS and ESI-MS/MS, and characterized its main fragments (Fig. 3). The ESI-MS/MS spectrum of GHK in positive ion mode (Fig. 3A) showed the pseudo-molecular ion of the parent peptide at *m/z* 341, one ion at *m/z* 323 (base peak), and one at *m/z* 195 $[MH-Lysine]^+$due to the formation of its b_3 and b_2 fragments, according to Roepstorff and Fohlman [13]. Subsequent loss of water and ammonia typical of amino acids gave rise to the formation of fragment ions at *m/z* 306 and 305. Fig. 3B shows the MS^3 spectrum of the product ion at *m/z* 306.

As previously observed in the reaction of carnosine and homocarnosine with ACR [8], the positive ion mode ESI-MS spectrum of the 1:1 GHK/ACR incubates gave a complex pattern of mono-, di- and tri-ACR adduction products (Fig. 4). Scheme 1 summarizes the reaction cascade of ACR with GHK and the structures of the adducts.

In the stoichiometric conditions used, in addition to the ion at *m/z* 341 $[GHK+H]^+$ due to the unreacted tripeptide and the one at *m/z* 171 due to its double-charged ion, the spectrum shows two main ions that can be reasonably attributed to (i) a mono-ACR dehydrated Michael adduct at *m/z* 379 $[GHK+ACR-H_2O+H]^+$, (ii) a di-ACR adduct at *m/z* 435 $[GHK+2ACR-H_2O+H]^+$ (with the ion at *m/z* 218 very likely due to its $[GHK+2H]^{2+}$ double-charged ion), the ion at *m/z* 453 $[GHK+2ACR+H]^+$ (with its sodium adduct at *m/z* 475 $[GHK+2ACR+Na]^+$) and, finally, to the three-ACR adducts at *m/z* 491 $[GHK+3ACR-H_2O+H]^+$, and *m/z* 509 $[GHK+3ACR+H]^+$.

To definitively characterize these main adducts, we analyzed the ions at *m/z* 379, 435 and 509 by ESI-MS/MS, and Fig. 5 and Table 1 show their spectra, together with the attribution of the fragment ions. The ESI-MS/MS spectrum of the ion at *m/z* 379 (Fig. 5A) had two fragment ions, the first diagnostic of a macrocyclic species, the second of an open-ring structure, isobaric with the macrocycle.

- The first at *m/z* 233 $[GHK+ACR-H_2O-Lysine+H]^+$ due to the neutral loss of a lysine, from the highly stabilized macrocyclic structure A2 generated by Michael addition of the electrophilic C-3 of ACR to the N^τ of the histidine residue, with subsequent formation of a Schiff base between ACR and the amino group of Gly and
- The second at *m/z* 185 $[GHK+ACR-H_2O-GH+H]^+$, consistent with fragmentation of the Schiff base **A1′** formed by condensation of the terminal amino group of the Lys residue with the carbonyl group of ACR.

The ESI-MS/MS spectrum of the pseudo-molecular ion at *m/z* 435 $[GHK+2ACR-H_2O+H]^+$ (Fig. 5B) shows the fragment at *m/z* 417 corresponding to the $[M-H_2O+H]^+$ ion as base peak. Minor but significant fragments from $[M+H]^+$ at *m/z* 435 relative to two isobaric species are detectable in the spectrum. In detail:

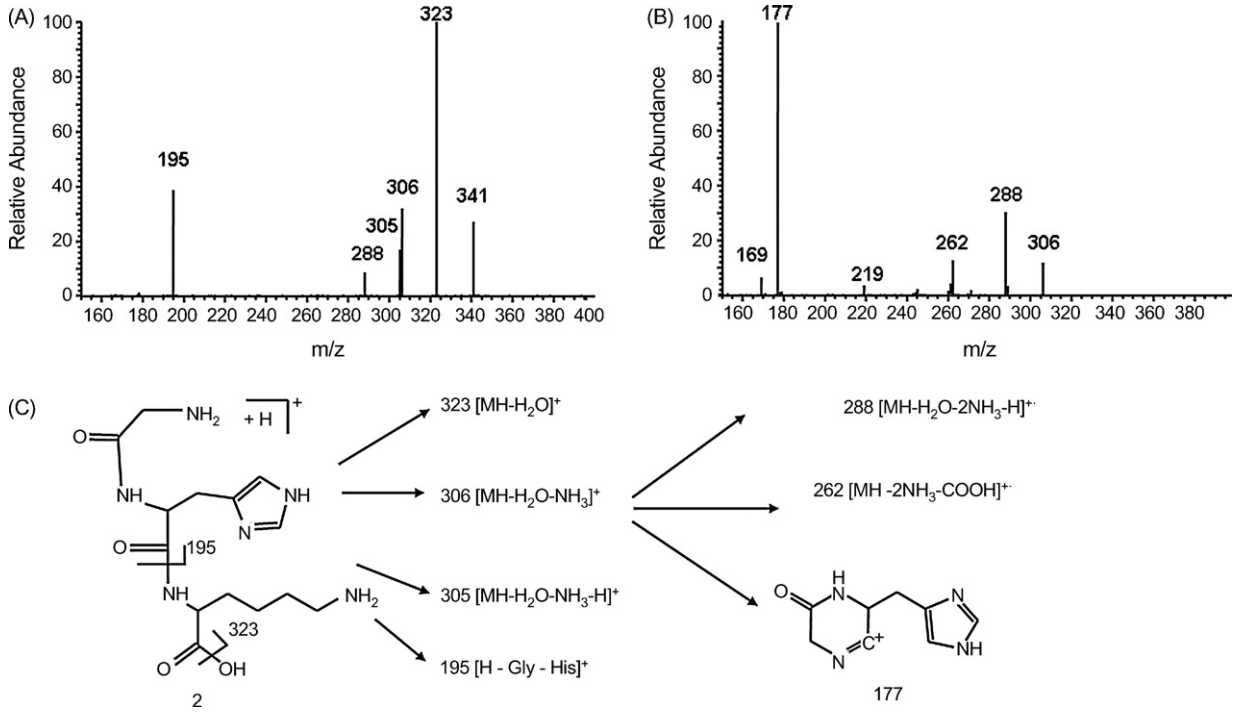

Fig. 3. (A) ESI-MS/MS spectrum of the pseudo-molecular ion of GHK at *m/z* 341, (B) ESI-MS/MS spectrum of the fragment ion of GHK at *m/z* 306 and (C) attribution of the main fragment ions identified.

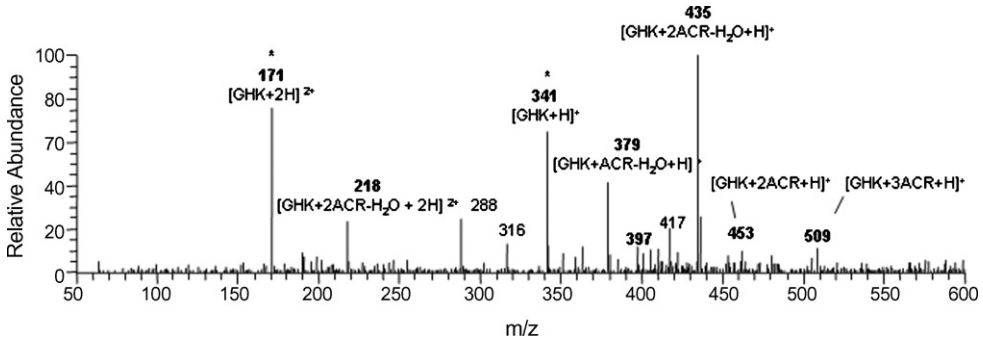

Fig. 4. Positive-ion ESI mass spectra of a 1:1 ACR/GHK reaction mixture after (a) 4 h incubation.

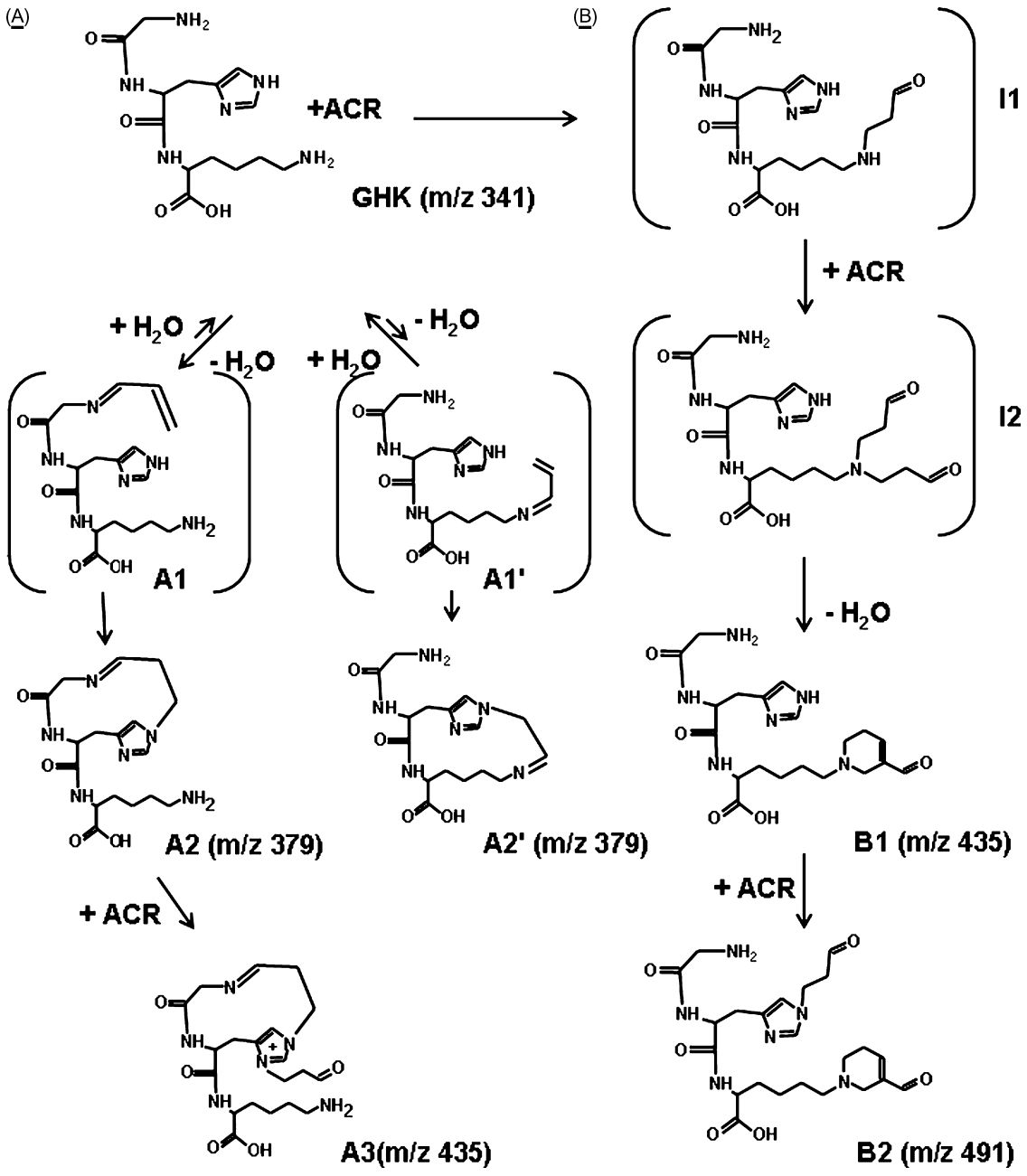

Scheme 1. Cascade of reaction between GHK and ACR and structures of the intermediates and final adducts formed.

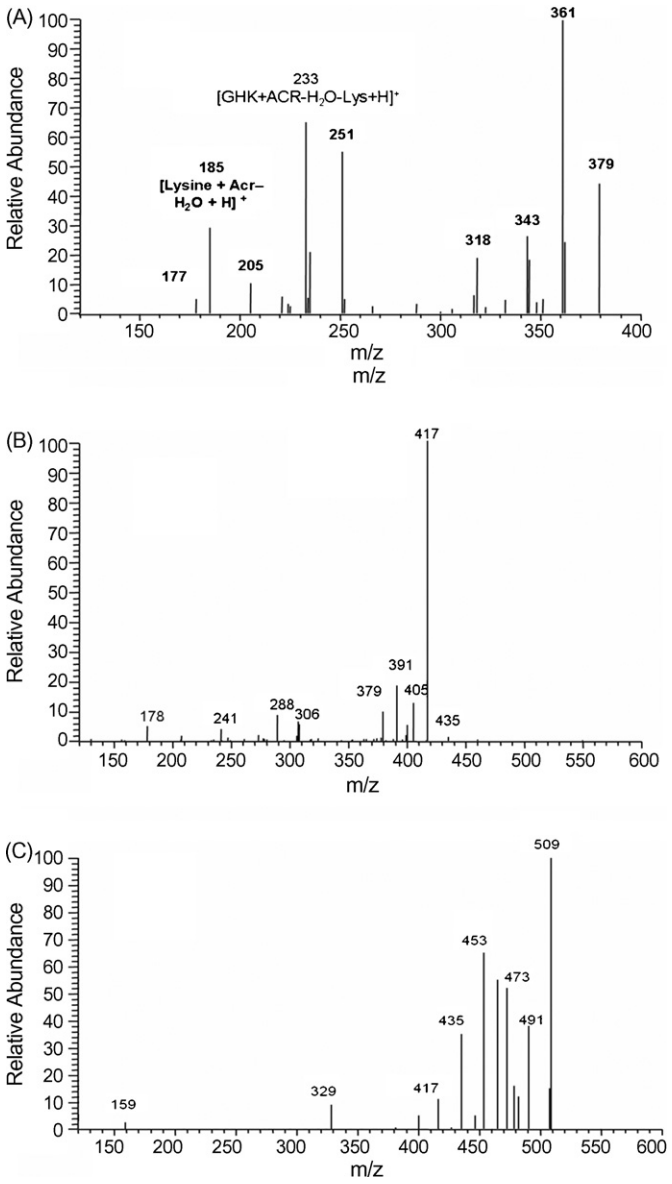

Fig. 5. ESI-MS^2 spectra of the $[M+H]^+$ ions at m/z 379, 435 and 509.

- The ions at m/z 379 $[M-ACR+H]^+$ from the neutral loss of an ACR moiety from the mono-ACR adduct through a typical retro-Michael reaction, at m/z 391 $[MH-CH_3HC=O]$ and one at m/z 307 $[MH-Lys]^+$ from the molecular species generated by the addition of a second ACR molecule to the imidazole group of the macrocyclic mono-ACR adduct **A2** to give **A3**.
- The ions at m/z 405 $[MH-H_2C=O]$ and m/z 241 $[Lys+2ACR-H_2O+H]^+$ are due to cleavage of the GHK/FDP adduct **B1**, which arises from the incorporation of two ACR molecules by Michael addition into the terminal amino group of the Lys residue, followed by aldol condensation and dehydration.

The ion at m/z 509, barely detectable in the ESI-MS spectrum, represents the hydrated form of the adduction product **B2** due to the addition of a third ACR to the imidazole ring of the adduct **B1** (fragment ions in Table 1).

Table 1
ESI-MS/MS data relative to the fragmentation of the pseudo-molecular ions at m/z 379, 435 and 509: fragment ions, relative intensity and attribution

Pseudo-molecular ion	Fragment ions (m/z)	Relative intensity (%)	Attribution
m/z 379	362	23	$[MH-NH_3]^+$
	361	100	$[MH-H_2O]^+$
	344	18	$[MH-H_2O-NH_3]^+$
	343	26	$[MH-H_2O-NH_3-H]^+$
	318	19	$[MH-CO_2-NH_3]^+$
	317	6	$[MH-CO_2-H_2O]^+$
	251	54	$[MH-lys]^+$
	233	64	$[MH-lys-H_2O]^+ = b_2$
	205	10	$[MH-lys-H_2O-CO]^+ = a_2$
	185	28	$[Lysine+ACR-H_2O+H]^+ = y''_1$
	128	10	$[lys]^+$
m/z 435	417	100	$[MH-H_2O]^+$
	405	12	$[MH-HCHO]^+$
	391	19	$[MH-CO_2]^+$
	379	10	$[MH-ACR]^+$
	307	7	$[MH-lys]^+$
	289	9	$[MH-lys-H_2O]^+$
	241	4	$[Lysine+2ACR-H_2O+H]^+ = y''_1$
	178	5	$[Hglyhis-NH_3]^+$
m/z 509	508	15	$[M]^{+\cdot}$
	491	38	$[MH-H_2O]^+$
	479	16	$[MH-HCHO]^+$
	473	52	$[MH-2H_2O]^+$
	465	55	$[MH-CO_2]^+$
	453	65	$[MH-ACR]^+$
	447	5	$[MH-CO_2-H_2O]^+$
	435	35	$[MH-ACR-2H_2O]^+$
	417	10	$[MH-ACR-2H_2O]^+$
	400	5	$[MH-ACR-2H_2O-NH_3]^+$

3.3. Reaction cascade

On the basis of the mass spectrometry findings, two reaction cascades can be proposed: in the first (Scheme 1, pathway A), the first ACR molecule is added at the terminal amino group of Gly by reversible formation of a Schiff base through condensation and dehydration of the aldehyde carbonyl of the ACR moiety, followed by intramolecular Michael addition at the N^τ of the histidine moiety (**A1**), leading to the formation of the stabilized macrocyclic product **A2**. The addition of a second molecule of ACR to **A2** generates the 13-member cyclic compound **A3**.

In the second reaction cascade (Scheme 1, pathway B) two molecules of ACR react in a sequential Michael reaction with the terminal amino group of the lysyl residue (products **I1** and **I2**) of GHK, giving rise, after intra-molecular aldol condensation and dehydration, to the formation of the *N*-(3-formyl-3,4-dehydropiperidino) derivative (m/z 435, adduct **B1**), already observed by Uchida et al. as the modification reaction product between lysine and ACR [2]. The product **B2** arises from the Michael addition of a third ACR molecule to the N^τ of histidine of product **B1** (m/z 491).

3.4. Theoretical analyses

A modeling study was done to clarify why the mechanism of ring closure of the macrocycle **A1** involved the formation of the Schiff base between the aldehyde carbonyl of ACR and the N amino group of Gly only, and not the Lys terminus. We therefore considered the intermediate model g (Fig. 6) in which the adduction takes place in the nucleophilic and basic imidazole groups of His, as observed by Uchida et al. [14], and the carbonyl group of the ACR moiety is still free, so we could evaluate the different facility of condensation with both the aminic termini.

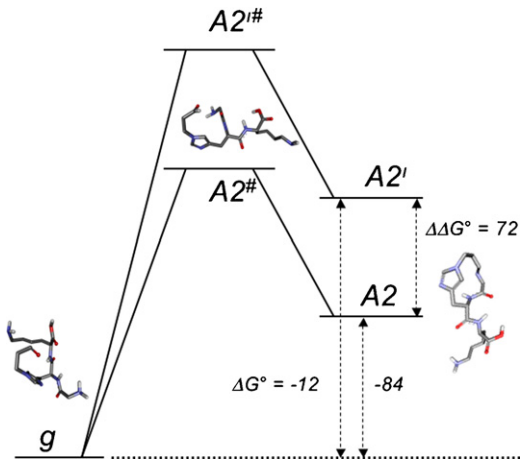

Fig. 6. Graphical representation of the energy differences (kcal/mol) between A2 and A2′.

GHK and g are very flexible molecules, with several rotatable bonds (degrees of freedom) giving origin to a large number of possible conformations. The g low-energy conformation in water has an unfolded structure, with $NH_2\cdots$C=O distances of 6.68 for NGly and 4.17 Å for N^{ζ}Lys. The g derivative should have a different conformation, to bring the NH_2 groups of Gly (or Lys) close to the C=O group and allow closure of the macrocycle. To find the best tri-dimensional structures (spatial arrangement) of the reaction transition state we analyzed the structure with Gaussian03 at the B2LYP/6-31G(d) level of theory.

Analysis of the energy levels indicated that the required conformational changes are possible for both Gly and Lys, giving rise to two conformers with $NH_2\cdots$C=O distances of 6.68 and 4.17 Å for NGly and N^{ζ}Lys, with a predominance of the NGly$\cdots$C=O intermediate (A2$^{\#}$), which has lower energy than the NLys$\cdots$C=O (A2′$^{\#}$) intermediate (ΔE of 6.28 kcal/mol). This was also confirmed by the molecular orbital's (MO) positions and energies. For both the A2′$^{\#}$ and A2$^{\#}$ intermediates, the lowest unoccupied molecular orbital (LUMO) is located over the aldehyde moiety, while the highest occupied molecular orbital (HOMO) is centered over the Gly, indicating that this residue is preferred for the Schiff base formation and subsequent ring closure. The HOMO–LUMO energy gap is also lower for A2$^{\#}$, indicating that this intermediate is softer than A2′$^{\#}$ (HOMO–LUMO gaps, respectively 8.96 and 9.22 eV for A2$^{\#}$ and A2′$^{\#}$). This is particularly important since soft molecules undergo unimolecular reactions more readily than hard ones, so a small energy gap favors the progress of the reaction. However, this conformational change is followed by the ring closure, a process favored by the superimposed MOs. The energies of the resulting macrocycles A2′ and A2 are again separated by about the same energy gap as for the respective intermediates (ΔE of 6.27 kcal/mol) (Fig. 6). The A2$^{\#}$ transition state leads, in any event, to an optimal superimposition of the glycine HOMO and the aldehyde LUMO, favoring ring closure and consequently the preferred formation of the macrocyclic intermediate A2. The selective formation of A2 is further substantiated by the vast difference in the ΔG^0 for the two reactions (−83.75 and −11.53 for A2 and A2′), that gives rise to a $\Delta\Delta G^0$ of ∼72 kcal/mol, which shifts the reaction towards the univocal formation of A2.

In conclusion, it is interesting that the mono-ACR adduct of GHK was detectable only in the first reaction cascade, that leads to the macrocycle A2 through the formation of a Schiff base intermediate at the Gly residue, as substantiated by the theoretical calculations, followed by ring closure through Michael intramolecular addition. This adduct can undergo subsequent Michael addition of ACR at the second N atom of the imidazole group, giving rise to the formation of the cationic product A3 stabilized by charge delocalization.

In the alternative pathway of adduction (B, Scheme 1), the first step of conjugation is dominated by the Michael addition of ACR at the Lys residue (not to Gly, otherwise we drop into the pathway A; the formation of an iminic product instead of a Michael addition is favored due to the stabilizing effect of the macrocycle formation). The mono-ACR Michael adduct is undetectable in the MS spectrum, since this ACR/GHK adduct at the Lys residue immediately traps a second ACR molecule to give the highly stabilized FDP derivative B1 after aldol condensation and irreversible dehydration. This product can add a third ACR molecule at the imidazole group to give the final adduct B2.

In the absence of kinetic quantitative data on pathways A and B, we cannot establish which of the pathways prevails in test-tube conditions, and extrapolation of this finding to the *in vivo* situation is even more difficult. However, hypothetically pathway B should be favored by a molar excess of ACR, while at low concentrations pathway A prevails.

4. Conclusions

This study found that the tripeptide GHK can quench the highly cytotoxic aldehyde ACR. At an equimolecular ratio, GHK can add up to two or three molecules of ACR giving rise to the formation of a set of intermediate and final products. These compounds, if formed *in vivo*, are easily excreted from the body as such because they are highly hydrophilic, or else they are eliminated as inactive metabolites after rapid hydrolysis. In addition, the proposed reaction cascade acquires biological relevance if we bear in mind that GSH, the main endogenous ACT trapping agent *in vivo*, can in several pathological situations be markedly depleted, and unable to counteract carbonyl stress [3]. Thus, in this case the detoxifying intervention of GHK can attenuate or prevent the formation of ACR/protein adducts which cause either inactivation of the biological target or the formation of immunogenic epitopes [15].

From an analytical view the tandem ESI-MS technique, under relatively simple conditions (infusion experiments) enables to obtain a rapid and detailed profiling of the products of the reaction of a peptide with ACR (i.e. to locate the position and deduce the modified residues within it). In addition it may be considered the technique of choice for the design and development of even more efficient quenchers against endogenous/exogenous α,β-unsaturated aldehydes.

Finally the combination of the ESI-MS data with computational evidence provide a strong support to the proposed mechanism of ACR detoxification in vitro.

References

[1] H. Esterbauer, R.J. Schaur, H. Zollner, Free Rad. Biol. Med. 11 (1991) 81–128.
[2] K. Uchida, M. Kanematsu, Y. Morimitsu, T. Osawa, N. Noguchi, E. Niki, J. Biol. Chem. 273 (1998) 16058–16066.
[3] L. Wood, A. Khan, S.R. Kulow, S.A. Mahamood, J.R. Moskal, Brain Res. 1095 (2006) 190–199.
[4] U. Nair, H. Bartsch, J. Nair, Free Rad. Biol. Med. 43 (2007) 1109–1120.
[5] Y.S. Park, K. Layoung, Y. Misonou, R. Takamiya, T. Motoko, R.F. Michael, N. Taniguchi, Arterioscler. Thromb. Vasc. Biol. 27 (2007) 1319–1325.
[6] L. Pickart, Lymphokines 8 (1983) 425–446.
[7] G. Beretta, R. Artali, L. Ragazzoni, M. Panigati, R. Maffei Facino, Chem. Res. Toxicol. 20 (2007) 1309–1314.
[8] M. Carini, G. Aldini, G. Beretta, E. Arlandini, R. Maffei Facino, J. Mass Spectrom. 38 (2003) 996–1006.
[9] P. Ren, J.W. Ponder, J. Phys. Chem. B 107 (2003) 5933–5947.
[10] P. Ren, J.W. Ponder, J. Comput. Chem. 23 (2002) 1497–1506.

[11] M.J. Frisch, G.W. Trucks, H.B. Schlegel, G.E. Scuseria, M.A. Robb, J.R. Cheeseman, J.A. Montgomery Jr., T. Vreven, K.N. Kudin, J.C. Burant, J.M. Millam, S.S. Iyengar, J. Tomasi, V. Barone, B. Mennucci, M. Cossi, G. Scalmani, N. Rega, G.A. Petersson, H. Nakatsuji, M. Hada, M. Ehara, K. Toyota, R. Fukuda, J. Hasegawa, M. Ishida, T. Nakajima, Y. Honda, O. Kitao, H. Nakai, M. Klene, X. Li, J.E. Knox, H.P. Hratchian, J.B. Cross, V. Bakken, C. Adamo, J. Jaramillo, R. Gomperts, R.E. Stratmann, O. Yazyev, A.J. Austin, R. Cammi, C. Pomelli, J.W. Ochterski, P.Y. Ayala, K. Morokuma, G.A. Voth, P. Salvador, J.J. Dannenberg, V.G. Zakrzewski, S. Dapprich, A.D. Daniels, M.C. Strain, O. Farkas, D.K. Malick, A.D. Rabuck, K. Raghavachari, J.B. Foresman, J.V. Ortiz, Q. Cui, A.G. Baboul, S. Clifford, J. Cioslowski, B.B. Stefanov, G. Liu, A. Liashenko, P. Piskorz, I. Komaromi, R.L. Martin, D.J. Fox, T. Keith, M.A. Al-Laham, C.Y. Peng, A. Nanayakkara, M. Challacombe, P.M.W. Gill, B. Johnson, W. Chen, M.W. Wong, C. Gonzalez, J.A. Pople, Gaussian 03, Revision C. 02, Wallingford, CT, Gaussian, Inc., 2004.
[12] A. Gugliucci, N. Lunceford, E. Kinugasa, H. Ogata, J. Schulze, S. Kimura, Clin. Chim. Acta 56 (2006) 1201–1206.
[13] P. Roepstorff, J. Fohlman, Biochem. Mass Spectrom. 11 (1984) 601.
[14] K. Uchida, M. Kanematsu, K. Sakai, T. Matsuda, N. Hattori, Y. Mizuno, D. Suzuki, T. Miyata, N. Noguchi, E. Niki, T. Osawa, PNAS 95 (1998) 4882–4887.
[15] G. Aldini, I. Dalle-Donne, R.M. Facino, A. Milzani, M. Carini, Med. Res. Rev. 27 (2007) 817–868.